

# Elastic Contact Analysis of Shot-Peened Rough Surfaces

Wanlin Dai <sup>†</sup> , Weike Yuan <sup>†</sup> and Gangfeng Wang <sup>\*†</sup> 

Department of Engineering Mechanics, SVL and MMLL, Xi'an Jiaotong University, Xi'an 710049, China

\* Correspondence: wanggf@mail.xjtu.edu.cn

† These authors contributed equally to this work.

**Abstract:** Shot peening can effectively improve the mechanical performance of metal components, and thus has been widely employed in the engineering field. During the processing, the surface roughness of treated components will be completely changed, which could strongly affect their tribological behavior. However, few of the existing contact models are directed toward the rough surfaces generated by shot peening. In this study, the normal contact response between a shot-peened surface and a rigid plane is investigated based on the finite element method and the recently developed incremental contact model. The elastic contacts of the rough surfaces experimentally measured on three different shot-peened specimens are considered. Contrary to the conventional rough contact models, it is found that the dependence of the external load on the real contact area for the shot-peened surfaces is not at all linear, even for light loads. The slope of the area–load curve significantly varies at two transition points, which are intrinsically linked to the special structure of shot-peened surfaces.

**Keywords:** shot peening; rough surface; contact mechanics; finite element method



**Citation:** Dai, W.; Yuan, W.; Wang, G. Elastic Contact Analysis of Shot-Peened Rough Surfaces. *Lubricants* **2022**, *10*, 331. <https://doi.org/10.3390/lubricants10120331>

Received: 24 September 2022

Accepted: 14 November 2022

Published: 24 November 2022

**Publisher's Note:** MDPI stays neutral with regard to jurisdictional claims in published maps and institutional affiliations.



**Copyright:** © 2022 by the authors. Licensee MDPI, Basel, Switzerland. This article is an open access article distributed under the terms and conditions of the Creative Commons Attribution (CC BY) license (<https://creativecommons.org/licenses/by/4.0/>).

## 1. Introduction

Shot peening is a well-established surface treatment technique that can significantly enhance the surface hardness, fatigue life, and stress corrosion resistance of metallic components [1–4]. In this process, a group of high-speed pellets is used to randomly impact the material surface, inducing severe plastic deformation in the near-surface layer. Naturally, the surface topography is fully altered in view of substantial overlapped residual indentations. Such characteristic surface roughness could bring in undesirable effects on the functionality and life of components, and play a critical role in many physical phenomena, such as adhesion, friction, wear, lubrication, etc. In particular, the contact performance of shot-peened solids intimately depends on the geometrical structures of their surfaces.

Since the middle of the last century, the rough surface contact problem has always been the focus in the field of contact mechanics, and numerous approaches using different descriptions of rough surfaces have been developed to deal with this issue [5,6]. For example, Archard [7] modeled a rough surface as spherical protuberances covered with even smaller spheres. In the famous multi-asperity contact model by Greenwood and Williamson (GW) [8], the rough surface was treated to be composed of hemispherical asperities with identical curvature radii and with their heights following a Gaussian or exponential distribution. Furthermore, Nayak [9,10] used the stochastic process theory to analyze the rough surface, which was modeled as a two-dimensional isotropic Gaussian random process. Based on Nayak's method, Bush et al. [11] presented a complete statistical contact model by adopting paraboloids with randomly distributed curvatures and heights to approximate the asperities. This model was later extended to the contact of anisotropic rough surfaces [12]. Apart from the statistical description, Majumdar and Bhushan [13] proposed the fractal characterization of surface roughness and assumed that the rough surface can be described by the Weierstrass–Mandelbrot function. In the scaling theory of Persson [14], the power spectral density of the rough surface was required for

determining the real contact area under a given load. According to these conventional contact models, the real contact area is generally proportional to the normal load for large surface separation [15].

In spite of the tremendous development on the modeling of rough surface contact, very few models are applicable to the case of shot-peened surfaces. This is because the unique surface roughness induced by shot-peening processing does not meet the assumptions adopted in the aforementioned contact models. Specifically, the shape of the asperities of shot-peened surfaces is far from the approximation of a sphere or paraboloid, and the distribution of the surface height is usually non-Gaussian [16]. Therefore, modeling the contact of such kinds of rough surfaces is still an open task.

The finite element method (FEM) is a direct and robust approach for addressing the contact of general rough surfaces. By employing the fully three-dimensional finite element analysis, both the elastic and elastoplastic contact problems for self-affine fractal rough surfaces have been successfully solved [17,18]. In addition, a finite element simulation for the contact of Gaussian random rough surfaces accounting for strain gradient plasticity was achieved [19]. In these studies, it was also found that the real contact area linearly increases with the applied load, while the slope depends on the material properties. Recently, Wang et al. [20,21] developed an incremental method to analyze the contact of general rough surfaces. This method is not confined to the isotropic Gaussian surfaces and does not demand the asperities to be close to quadratic surfaces. It is assumed that the contact of rough surfaces is equivalent to the accumulation of identical circular contacts with radii estimated from the total contact area and the number of contact patches, which are directly obtained from the truncation sections of the rough surface at different heights. In addition, the contact responses of elastic and elastoplastic rough surfaces with non-Gaussian height distributions can be calculated by applying the boundary element method (BEM) [22,23].

In this paper, we aim to tackle the elastic contact problem for the peculiar rough surfaces generated by shot peening. The outline of this paper is organized as follows: In Section 2, several surface specimens were prepared by using shot-peening processing, and their morphologies were experimentally measured. In Section 3, the elastic contacts of the prepared shot-peened rough surfaces with a rigid flat were analyzed by the finite element method and the incremental contact model by Wang et al. [20,21]. Finally, Section 4 presents the relationship between the real contact area and applied load for these shot-peened surfaces, which shows a clear difference from the traditional intuition of linearity.

## 2. Sample Preparation and Experimental Measurement

Almen strips ( $76.1 \times 18.95 \times 1.295$  mm) were prepared to generate surface specimens. Three shot-peened rough surfaces (A, B, and C) with 100% surface coverage were generated using a pneumatic shot-peening machine. Surfaces A and B were peened by ASH 230 steel shots, and surface C was peened by ceramic shots. Both the steel and ceramic shots used in the peening procedures were spheroids. Table 1 shows the parameters of these two types of shots.

**Table 1.** Parameters of the shots used in the peening procedures.

Shot Material	Shot Diameter (mm)	Pressure (MPa)	Rate of Flow (kg/min)
ASH 230 steel	0.58–0.71	0.12	12
Ceramic	0.61–0.84	0.20	10

The topographies of the surface specimens were measured with a white light interferometer. As shown in Figure 1a–c, there are a large number of circular dimples on the surfaces, which are resulted from the random impacts of pellets. The distribution of these dimples on the surface is approximately isotropic. Sharp asperities were formed among the rims of the adjacent dimples. In this case, using a sphere or paraboloid to approximate these asperities is no longer valid, and the fractal characteristic is not clear either. Referring to the Cartesian coordinate system ( $o-xyz$ ), a three-dimensional rough surface can be represented

by  $z(x, y)$  where the reference plane  $z = 0$  is chosen at the mean plane of the rough surface. Figure 1d–f display the height distributions of surfaces A, B, and C, respectively. Obviously, the shot-peened rough surfaces are non-Gaussian.

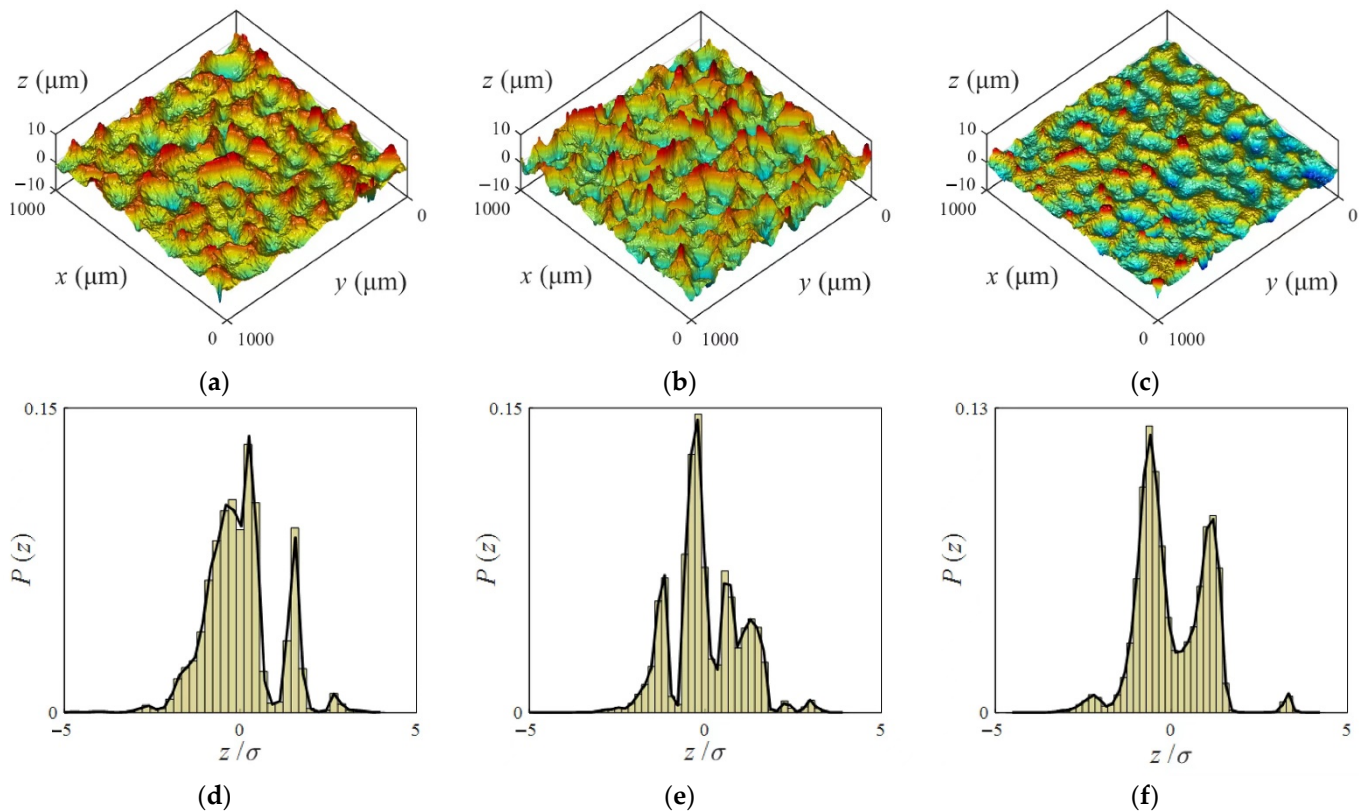


**Figure 1.** The topographies of the rough surfaces: (a) surface A, (b) surface B, (c) surface C; height distributions of the rough surfaces: (d) surface A, (e) surface B, (f) surface C.

These peculiar geometrical features of shot-peened rough surfaces lead to much difficulty to give an accurate theoretical prediction for the contact responses. In the next two sections, the experimentally measured surface topographies will be successively used to construct a finite element model in the contact simulations of shot-peened solids and estimate the number of contact patches and amount of contact area in the analysis using the incremental model.

### 3. Methods

#### 3.1. Finite Element Analysis

Finite element simulations for the contact between a shot-peened rough surface and rigid plane were performed using the commercial software ABAQUS/Explicit. As shown in Figure 2, a three-dimensional model was built with a side length of  $L$  and a height of  $H$  (where  $H = L/4$ ), which are far larger than the root mean square (RMS) roughness  $\sigma$  of the generated shot-peened surfaces. The nominal area of the contact problem is denoted by  $A_0$  ( $A_0 = L^2$ ). The upper surface of the substrate is rough, of which the topography is given by the height information measured in Section 2. The large flat plane that was used to compress the rough substrate under a normal load  $P$  was set as analytic rigid. The substrate with a shot-peened rough surface was assumed as homogeneous and isotropic. For the purely elastic contact, the linear elastic constitutive law was adopted with Young's modulus  $E$  and Poisson's ratio  $\nu$ . The values of the geometrical and mechanical parameters of the substrate are presented in Table 2. During the contact, friction and adhesion forces between the surfaces were not considered, and the bottom of the substrate was kept fixed.

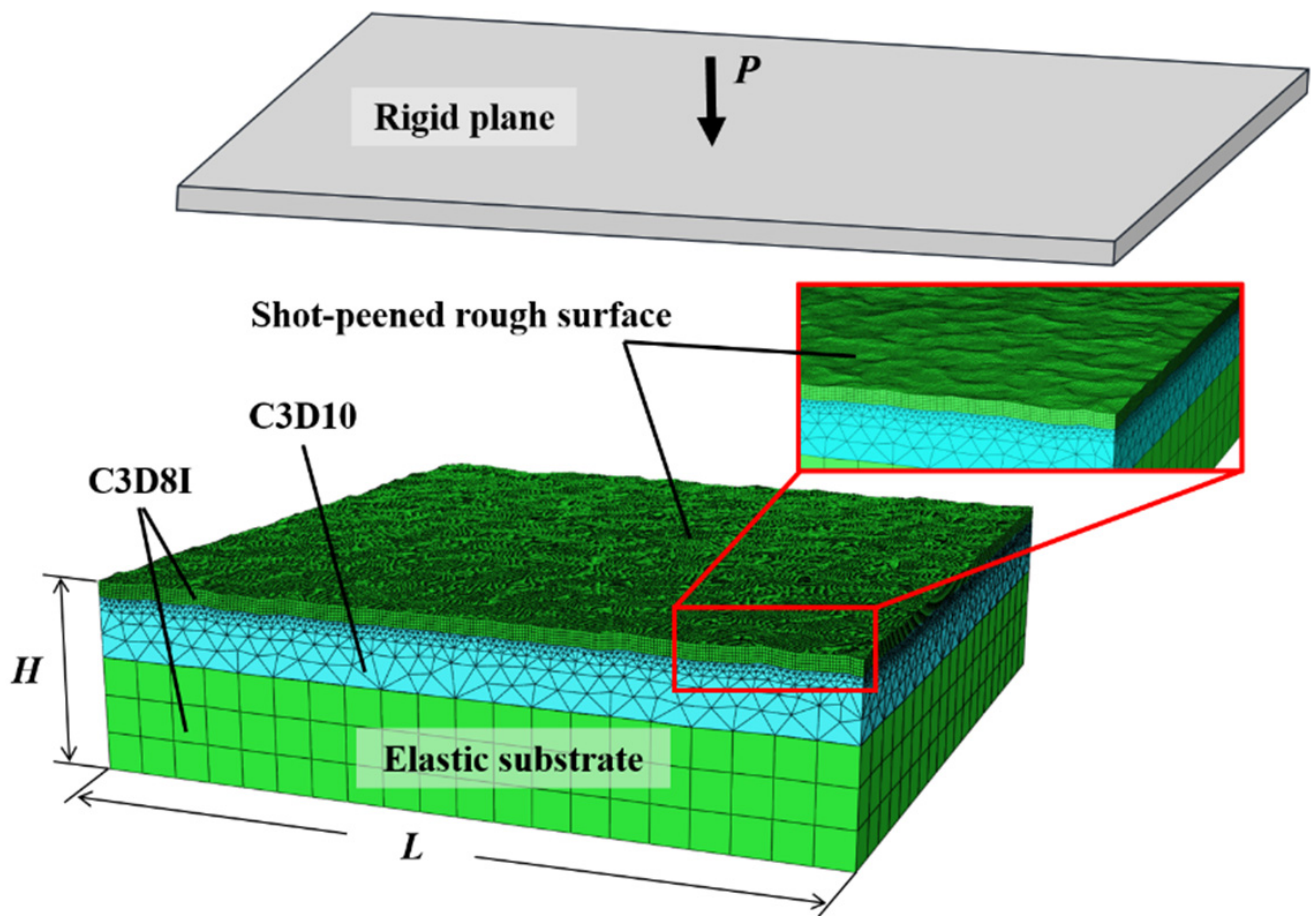


Figure 2. Finite element model of the shot-peened surface contact.

Table 2. Geometrical and mechanical parameters of the shot-peened rough solids.

Global Size		RMS Roughness, $\sigma$ ( $\mu\text{m}$ )			Mechanical Parameter	
$L$ (mm)	$H$ (mm)	Surface A	Surface B	Surface C	$E$ (GPa)	$\nu$
1.04	0.26	1.3803	1.9868	0.8808	91	0.3

In the simulations, the target rough surface was discretized by  $256 \times 256$  nodes with identical horizontal spacing. Associating with these surface nodes, the bulk close to the rough surface was finely meshed with eight-node linear hexahedral elements (C3D8I). For the bulk that was distant from the rough surface, the mesh also used C3D8I elements but was coarsened for reducing the computation cost. Ten-node quadratic tetrahedral elements (C3D10) were adopted for the mesh of the transitional bulk. In total, the number of elements in each of our simulations is about 668,600. Mesh convergence has been proven to ensure the accuracy of the simulation results.

### 3.2. Incremental Contact Model

The incremental equivalent approach proposed by Wang et al. [20,21] was used to analyze the contacts of shot-peened rough surfaces. According to this method, the geometrically truncated area of the rough surface at the specified height  $z$  is treated as the real contact area  $A$ . In addition, the contact patches are simplified by a group of equivalent circular patches, as shown in Figure 3, which have the same radius  $R$  given by

$$R = \sqrt{\frac{A(z)}{\pi N(z)}} \quad (1)$$

where  $A(z)$  is the total contact area and  $N(z)$  is the number of contact patches.

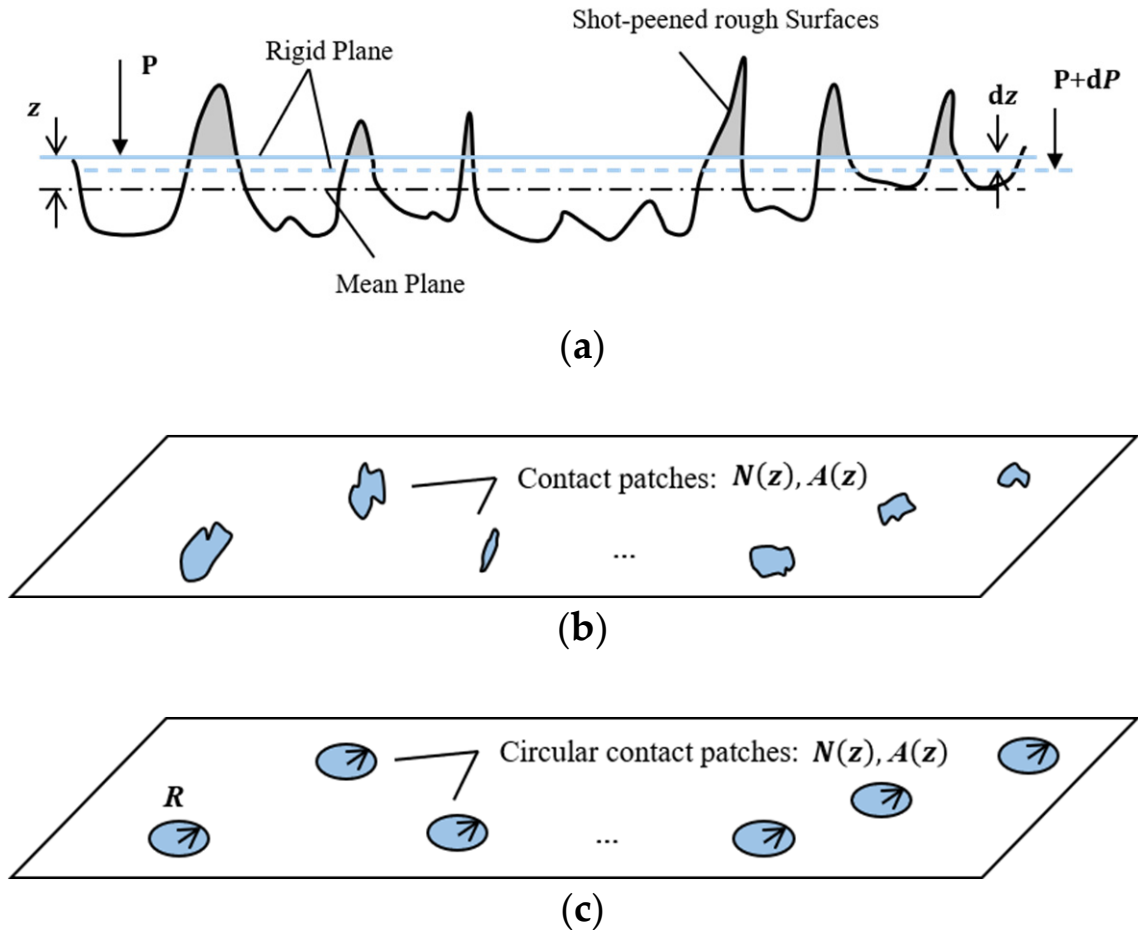


**Figure 3.** Schematic of the contact problem. (a) Contact of an elastic shot-peened rough surface with a rigid plane. (b) Discrete contact patches. (c) Equivalent circular contact patches.

For the decrement of the surface height  $dz$ , the increment of the normal load  $dP$  can be obtained by the current contact stiffness [20,21]:

$$dP = 2E^*RN(z)dz \quad (2)$$

where  $E^* = E/(1 - \nu^2)$ .

Then, substituting Equation (1) into Equation (2), the normal load  $P$  required for generating the total contact area  $A(z)$  is determined by integrating Equation (2) from  $z$  to infinity,

$$P = \int_z^\infty \frac{2}{\sqrt{\pi}} E^* \sqrt{A(z)N(z)} dz \quad (3)$$

For the shot-peened rough surfaces measured in Section 2, the total area  $A(z)$  and the number of contact patches  $N(z)$  at a different height  $z$  can be calculated through a numerical technique, as shown in Figures 4 and 5, respectively. Using a numerical integration approach, the load  $P$  can be calculated with the information of  $A(z)$  and  $N(z)$ . Consequently, the relationship between the normal load and contact area was established. More details about the incremental contact model may be referred to [20,21].

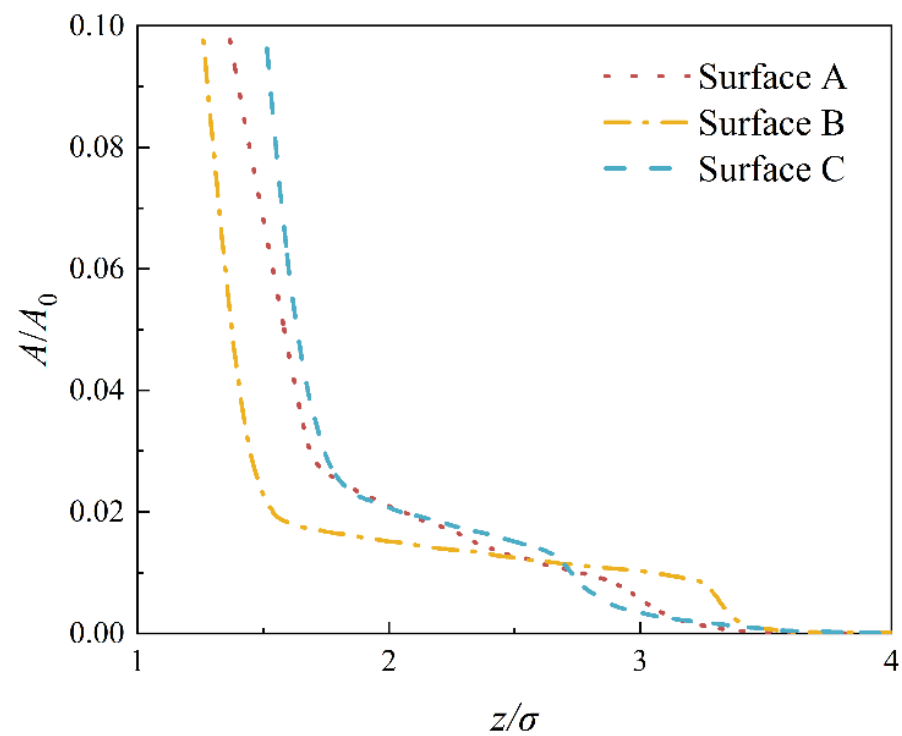


Figure 4. Variations of total contact area  $A/A_0$  with respect to  $z/\sigma$ .

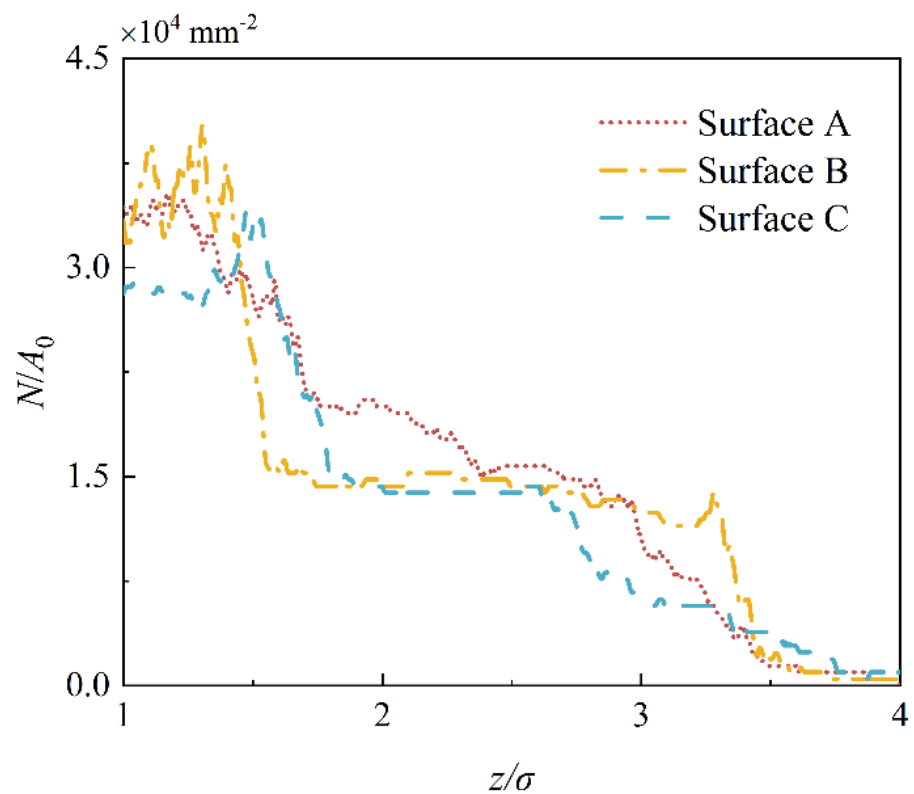


Figure 5. Variations of contact patch number  $N/A_0$  with respect to  $z/\sigma$ .

#### 4. Results and Discussion

Based on the finite element analysis and the incremental contact model of Wang et al. [20,21], we obtained the relationship between the real contact area and normal load for the measured shot-peened rough surfaces. Figures 6–8 display the dependences of the normalized load  $P/(E^*A_0)$  on the contact area fraction  $A/A_0$  for surfaces A, B, and C, respectively. It was

found that the prediction of the incremental contact model for the small contact area excellently agreed with the results of the finite element simulations. When the contact area is large, the incremental contact model become relatively less accurate. However, qualitative consistency with the simulation results still holds for the real contact area up to 10% of the nominal area.

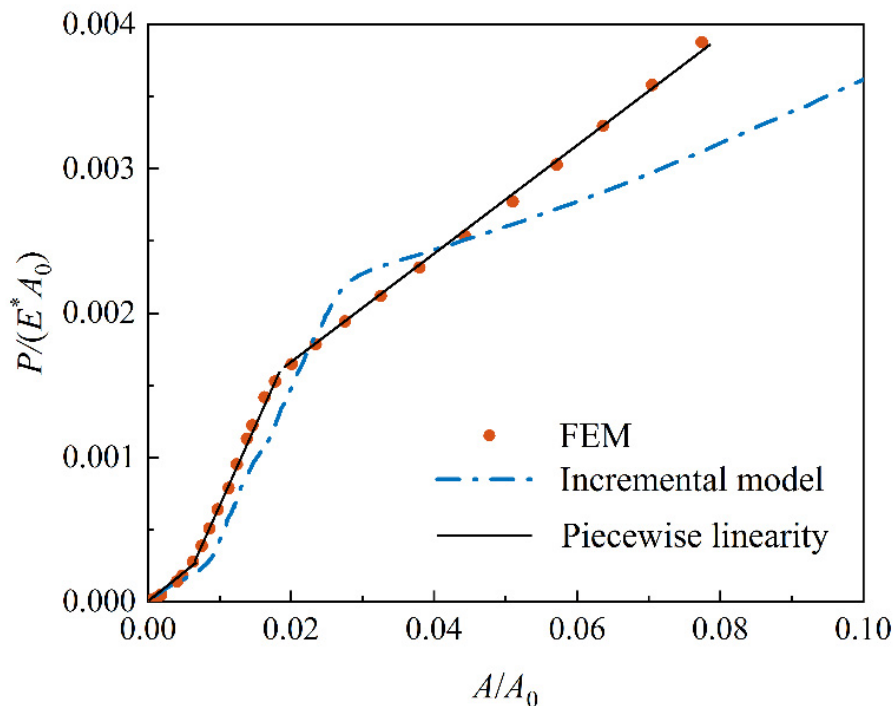


Figure 6. Dependence of the normalized load  $P/(E^*A_0)$  on the contact fraction  $A/A_0$  for surface A.

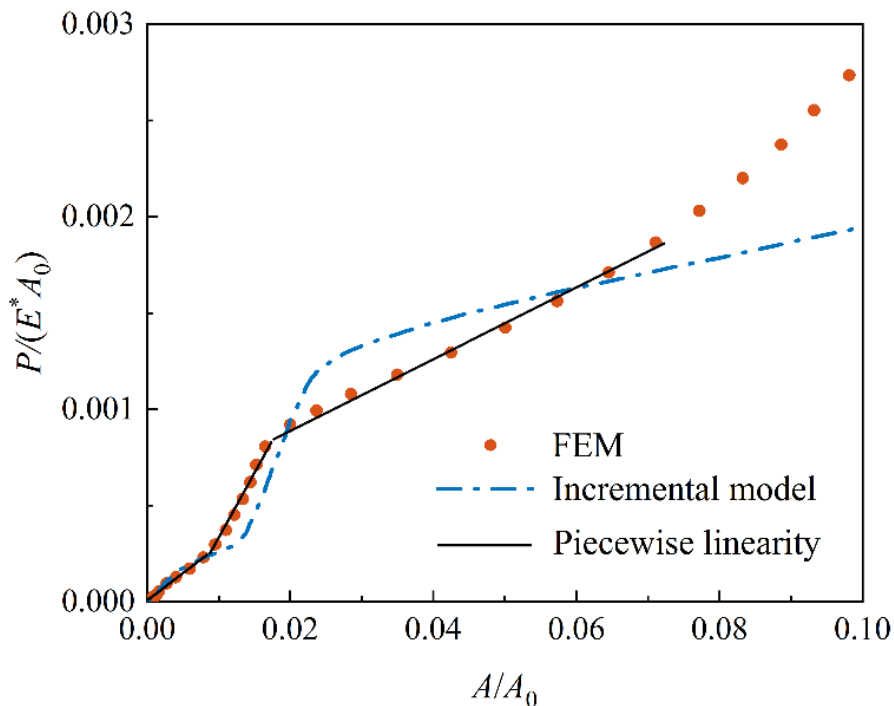
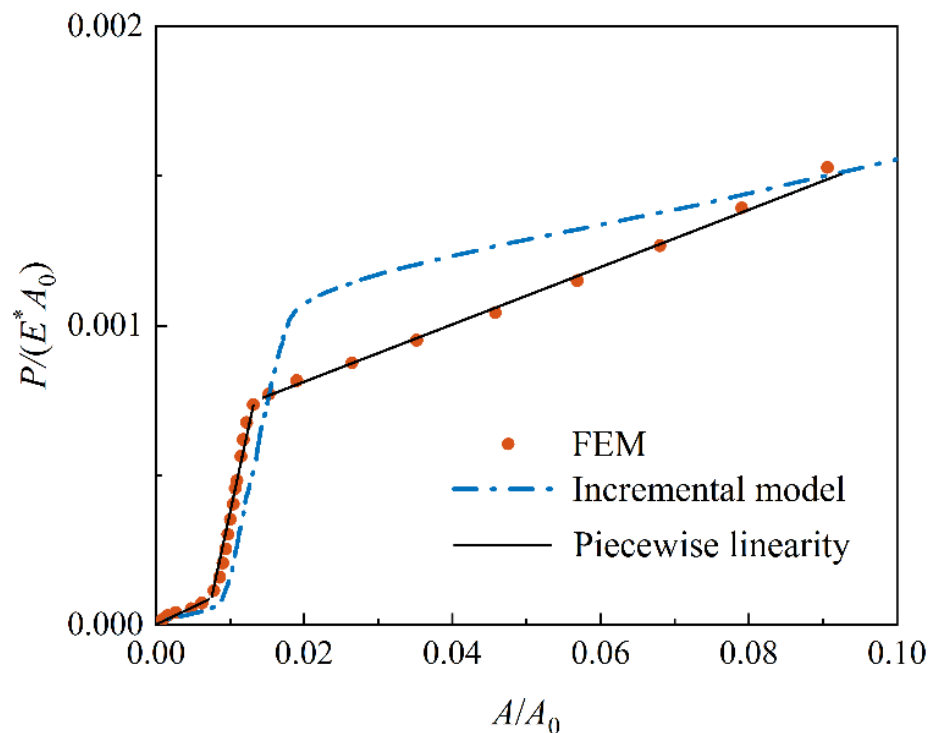


Figure 7. Dependence of the normalized load  $P/(E^*A_0)$  on the contact fraction  $A/A_0$  for surface B.



**Figure 8.** Dependence of the normalized load  $P/(E^*A_0)$  on the contact fraction  $A/A_0$  for surface C.

The linearity of the area–load relation has been repeatedly demonstrated in the conventional contact models of rough surfaces [15]. For the measured shot-peened rough surfaces, it is interesting to notice that the real contact area does not proportionally rise with the applied load, even for small loads. Approximately, the area–load relation can be considered as piecewise linear, and there are two remarkable transition points where the slope significantly changes. In the case of surface A, the slope increases after crossing the first transition point of  $A/A_0 = 0.9\%$ , and then declines after crossing the second transition point of  $A/A_0 = 1.8\%$ . For surfaces B and C, the transition points are  $A/A_0 = 0.6\%$ ,  $1.9\%$  and  $A/A_0 = 0.7\%$ ,  $1.4\%$ , respectively.

It is worth mentioning that such a trend of piecewise linearity is also revealed by the incremental contact model. In view of Equations (1) and (2), the slope of the area–load relation can be expressed by

$$\frac{dP}{dA} = -\frac{2E^* \sqrt{A(z)N(z)}}{\sqrt{\pi} dA(z)/dz} \quad (4)$$

Therefore, the slope is governed by the variation of the contact patch number and total contact area, which are directly related to the geometrical structure of the shot-peened surface. From Figures 4 and 5, it can be seen that both the total contact area  $A(z)$  and contact patch number  $N(z)$  significantly vary near these two transition points of slope change. Notably, the first derivative of  $A(z)$  (having a negative value) remarkably increases at the first transition point and sharply decreases at the second transition point. On the other hand, the contact patch number has evident increases near the transition points. Compared with the sharp decrease of  $dA(z)/dz$ , it seems that the influence of such a variation of  $N(z)$  is minor on the change of slope at the second transition point.

## 5. Summary

Based on the experimentally measured surface topography, the rough surface generated by shot peening is typically non-Gaussian and cannot be modeled by the classical description of paraboloidal asperity or fractal characterization. The elastic contact of shot-

peened rough surfaces was analyzed using the finite element method and the incremental approach proposed by Wang et al. [20,21]. It was found that the relationship between the real contact area and applied load is nonlinear even for small contact areas, which is quite different from the results of conventional contact models of rough surfaces. For the measured shot-peened surfaces, the area–load relation could be described well by the piecewise linear function. In the range considered in this work ( $A/A_0 < 10\%$ ), there are two significant transition points for the slope of the area–load curve. Essentially, the changes of slope are related to the surface features induced by shot peening. This study would be helpful for the understanding of the contact mechanics of special rough surfaces.

**Author Contributions:** Conceptualization, G.W.; methodology, W.D., W.Y. and G.W.; software, W.D.; validation, W.Y. and G.W.; formal analysis, W.D. and W.Y.; investigation, W.D. and W.Y.; resources, G.W.; data curation, W.D.; writing—original draft preparation, W.D. and W.Y.; writing—review and editing, W.Y. and G.W.; visualization, W.D. and W.Y.; supervision, G.W.; project administration, G.W.; funding acquisition, G.W. All authors have read and agreed to the published version of the manuscript.

**Funding:** This research was funded by the National Natural Science Foundation of China (grant no. 11525209).

**Conflicts of Interest:** The authors declare no conflict of interest.

## References

- Hu, Y.; Gong, C.; Yao, Z.; Hu, J. Investigation on the non-homogeneity of residual stress field induced by laser shock peening. *Surf. Coat. Technol.* **2009**, *203*, 3503–3508. [[CrossRef](#)]
- Bagherifard, S.; Slawik, S.; Fernández-Pariente, I.; Pauly, C.; Mücklich, F.; Guagliano, M. Nanoscale surface modification of AISI 316L stainless steel by severe shot peening. *Mater. Des.* **2016**, *102*, 68–77. [[CrossRef](#)]
- Wu, D.; Yao, C.; Zhang, D. Surface characterization and fatigue evaluation in GH4169 superalloy: Comparing results after finish turning; shot peening and surface polishing treatments. *Int. J. Fatigue* **2018**, *113*, 222–235. [[CrossRef](#)]
- Soyama, H. Comparison between the improvements made to the fatigue strength of stainless steel by cavitation peening, water jet peening, shot peening and laser peening. *J. Mater. Process. Technol.* **2019**, *269*, 65–78. [[CrossRef](#)]
- Taylor, R.I. Rough surface contact modelling—A Review. *Lubricants* **2022**, *10*, 98. [[CrossRef](#)]
- Vakis, A.I.; Yastrebov, V.A.; Scheibert, J.; Nicola, L.; Dini, D.; Minfray, C.; Almqvist, A.; Paggi, M.; Lee, S.; Limbert, G.; et al. Modeling and simulation in tribology across scales: An overview. *Tribol. Int.* **2018**, *125*, 169–199. [[CrossRef](#)]
- Archard, J.F. Elastic deformation and the laws of friction. *Proc. R. Soc. Lond.* **1957**, *243*, 190–205.
- Greenwood, J.A.; Williamson, J.B.P. Contact of nominally flat surfaces. *Proc. R. Soc. A* **1966**, *295*, 300–319.
- Nayak, P.R. Random process model of rough surfaces. *J. Lubr. Technol.* **1971**, *93*, 398–407. [[CrossRef](#)]
- Nayak, P.R. Random process model of rough surfaces in plastic contact. *Wear* **1973**, *26*, 305–333. [[CrossRef](#)]
- Bush, A.W.; Gibson, R.D.; Thomas, T.R. The elastic contact of a rough surface. *Wear* **1975**, *35*, 87–111. [[CrossRef](#)]
- Bush, A.W.; Gibson, R.D.; Keogh, G.P. Strongly anisotropic rough surfaces. *J. Tribol.* **1979**, *101*, 15–20. [[CrossRef](#)]
- Majumdar, A.; Bhushan, B. Fractal model of elastic-plastic contact between rough surfaces. *J. Tribol.* **1991**, *113*, 1–11. [[CrossRef](#)]
- Persson, B.N.J. Theory of rubber friction and contact mechanics. *J. Chem. Phys.* **2001**, *115*, 3840–3861. [[CrossRef](#)]
- Carbone, G.; Bottiglione, F. Asperity contact theories: Do they predict linearity between contact area and load? *J. Mech. Phys. Solids* **2008**, *56*, 2555–2572. [[CrossRef](#)]
- Bagherifard, S.; Ghelichi, R.; Guagliano, M. Numerical and experimental analysis of surface roughness generated by shot peened. *Appl. Surf. Sci.* **2012**, *258*, 6831–6840. [[CrossRef](#)]
- Hyun, S.; Pei, L.; Molinari, J.F.; Robbins, M.O. Finite-element analysis of contact between elastic self-affine surfaces. *Phys. Rev. E* **2004**, *70*, 026117. [[CrossRef](#)]
- Pei, L.; Hyun, S.; Molinari, J.F.; Robbins, M.O. Finite element modeling of elasto-plastic contact between rough surfaces. *J. Mech. Phys. Solids* **2005**, *53*, 2385–2409. [[CrossRef](#)]
- Song, H.; Van der Giessen, E.; Liu, X. Strain gradient plasticity analysis of elasto-plastic contact between rough surfaces. *J. Mech. Phys. Solids* **2016**, *96*, 18–28. [[CrossRef](#)]
- Wang, G.F.; Liang, X.M.; Yan, D. An incremental equivalent circular contact model for rough surfaces. *J. Tribol.* **2021**, *143*, 081503. [[CrossRef](#)]
- Wang, S.H.; Yuan, W.K.; Liang, X.M.; Wang, G.F. A new analytical model for the flattening of Gaussian rough surfaces. *Eur. J. Mech.-A/Solids* **2022**, *94*, 104578. [[CrossRef](#)]
- Tiwari, A.; Almqvist, A.; Persson, B.N.J. Plastic deformation of rough metallic surfaces. *Tribol. Lett.* **2020**, *68*, 129. [[CrossRef](#)]
- Pérez-Ràfols, F.; Almqvist, A. On the stiffness of surfaces with non-Gaussian height distribution. *Sci. Rep.* **2021**, *11*, 1863. [[CrossRef](#)] [[PubMed](#)]